

¹ The Morphological Diversification of Siphonophore Tentilla

³ Alejandro Damian-Serrano^{1,‡}, Steven H.D. Haddock², Casey W. Dunn¹

⁴ ¹ Yale University, Department of Ecology and Evolutionary Biology, 165 Prospect St.,
⁵ New Haven, CT 06520, USA

⁶ ² Monterey Bay Aquarium Research Institute, 7700 Sandholdt Rd., Moss Landing, CA
⁷ 95039, USA

⁸ [‡] Corresponding author: Alejandro Damian-Serrano, email: alejandro.damianserrano@
⁹ yale.edu

¹⁰ Abstract

¹¹ Siphonophores are free-living predatory colonial hydrozoan cnidarians found in every ocean
¹² of the world. Siphonophore tentilla (tentacle side branches) are unique biological structures
¹³ for prey capture, composed of a complex arrangement of cnidocytes (stinging cells) bearing
¹⁴ different types of nematocysts (stinging capsules) and auxiliary structures. Tentilla present
¹⁵ an extensive morphological and functional diversity across species. While associations
¹⁶ between tentilla form and diet have been reported, the evolutionary history giving rise to this
¹⁷ morphological diversity is largely unexplored. Here we examine the evolutionary gains and
¹⁸ losses of novel tentillum substructures and nematocyst types on the most recent siphonophore
¹⁹ phylogeny. Tentilla have a precisely coordinated high-speed strike mechanism of synchronous
²⁰ unwinding and nematocysts discharge. Here we characterize the kinematic diversity of this
²¹ prey capture reaction using high-speed video and find relationships with morphological
²² characters. Since tentillum discharge occurs in synchrony across a broad morphological
²³ diversity, we evaluate how phenotypic integration is maintaining character correlations across
²⁴ evolutionary time. We found that the tentillum morphospace has low dimensionality, we
²⁵ identified instances of heterochrony and morphological convergence, and generated hypotheses

²⁶ on the diets of understudied siphonophore species. Our findings indicate that siphonophore
²⁷ tentilla are phenotypically integrated structures with a complex evolutionary history leading to
²⁸ a phylogenetically structured diversity of forms which are predictive of kinematic performance
²⁹ and feeding habits.

³⁰ **Keywords**

³¹ Siphonophore, tentilla, nematocysts, character evolution

³² **Introduction**

³³ Siphonophores have fascinated zoologists for centuries for their extremely subspecialized
³⁴ colonial organization and integration. Today we have a comprehensive taxonomic coverage
³⁵ on the morphological diversity of this group due to the extensive work of siphonophore
³⁶ taxonomists in the past few decades (1–10), which has been elegantly synthesized in detailed
³⁷ synopsis (11). In addition, recent advances in phylogenetic analyses of siphonophores (13, 14)
³⁸ have provided a macroevolutionary context to interpret this diversity. With these assets in
³⁹ hand, we can now begin to study siphonophores from an orthogonal perspective, focusing on
⁴⁰ the diversity and evolutionary history of specific structures. Here we focus on one of such
⁴¹ structures: the tentilla. Like many cnidarians, siphonophore tentacles bear side branches
⁴² (tentilla) with nematocysts (Fig. 1). But unlike other cnidarians, most siphonophore tentilla
⁴³ are dynamic structures that react to prey encounters by rapidly unfolding the nematocyst
⁴⁴ battery to slap around the prey. This maximizes the surface area of contact between the
⁴⁵ nematocysts and the prey they fire upon. In addition, siphonophore tentilla present a
⁴⁶ remarkable diversity of morphologies (Fig. 2), sizes, and nematocyst complements (Fig. 3).
⁴⁷ Our overarching aim is to organize all this phenotypic diversity in a phylogenetic context,
⁴⁸ and identify the evolutionary processes that generated it.

⁴⁹ In (14), we collected the most extensive morphological dataset on siphonophore tentilla and
⁵⁰ nematocysts using state-of-the-art microscopy techniques, and expanded the taxon sampling

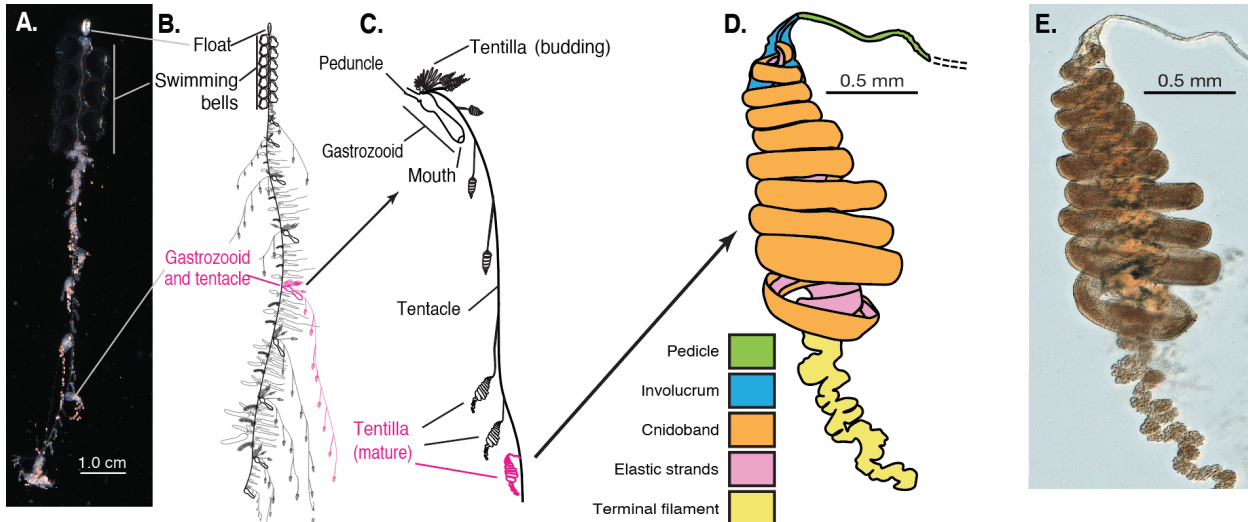


Figure 1: Siphonophore anatomy. A - *Nanomia* sp. siphonophore colony (photo by Catriona Munro). B, C - Illustration of a *Nanomia* colony, gastrozooid, and tentacle closeup (by Freya Goetz). D - *Nanomia* sp. Tentillum illustration and main parts. E - Differential interference contrast micrograph of the tentillum illustrated in D. Figure reproduced from Damian-Serrano et al. 2020 with permission.

of the phylogeny to disentangle the evolutionary history. The analyses we carried out led to novel, generalizable insights into the evolution of predatory specialization. The primary findings of that work were that generalists evolved from crustacean-specialist ancestors, and that feeding specializations were associated with distinct modes of evolution and character integration patterns. The work we present here is complementary to (14), showcasing a far more detailed account on the evolutionary history of tentilla morphology.

Nematocysts are unique biological weapons for defense and prey capture exclusive to the phylum Cnidaria. Mariscal ((15)) reported that hydrozoans have the largest diversity of nematocyst types among cnidarians. Among them, siphonophores present the greatest variety of types (12), and vary widely across taxa in which and how many types they carry on their tentacles (Fig. 3). Werner (16) noted that there are nine types of nematocyst found in siphonophores, of which four, anacrophore rhopalonemes, acrophore rhopalonemes, homotrichous anisorhizas, and birhopaloids, are unique to them. Heteroneme and haploneme nematocysts serve penetrant and entangling functions, while rhopalonemes and desmonemes

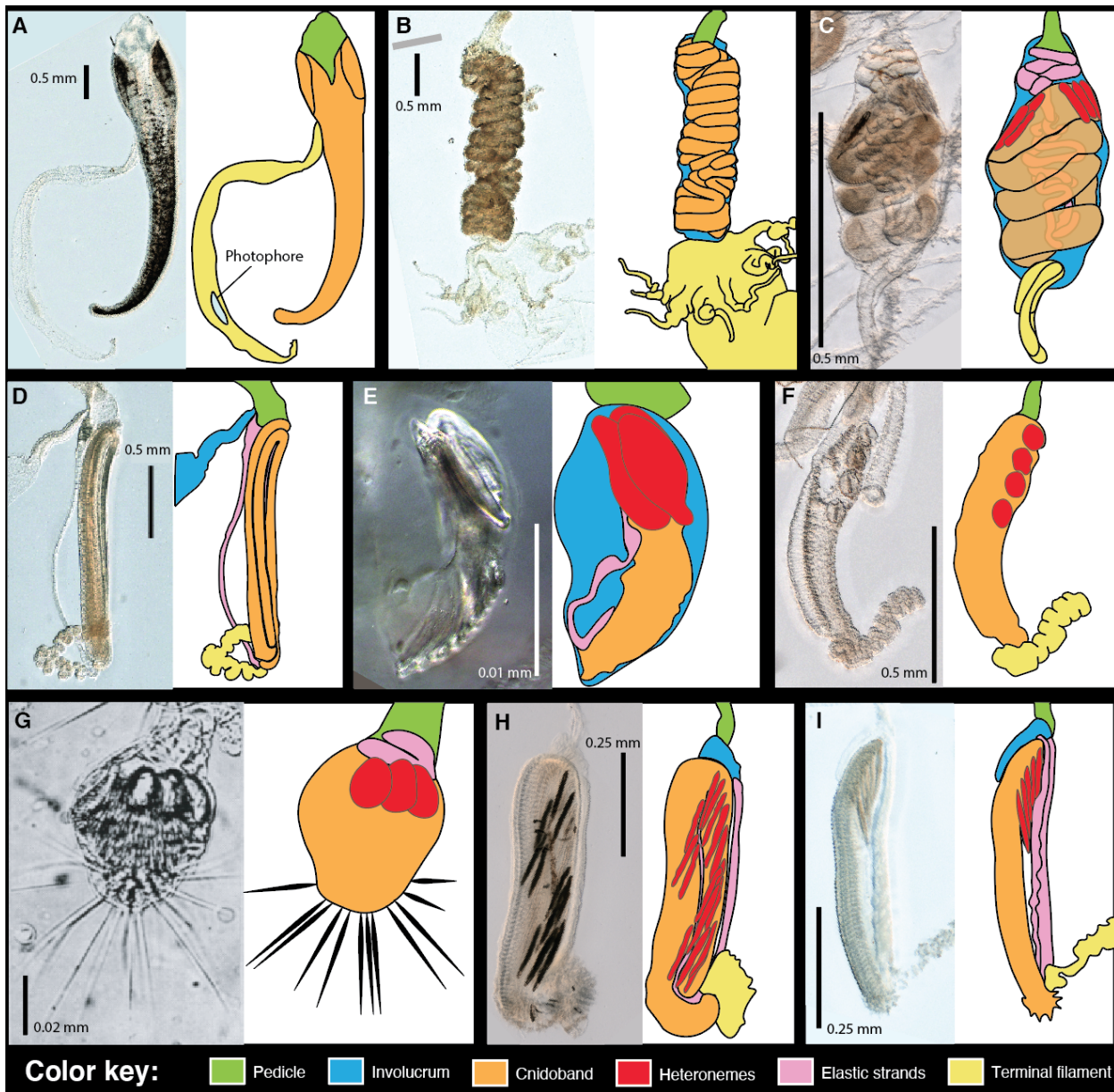


Figure 2: Tentillum diversity. The illustrations delineate the pedicle, involucrum, cnidoband, elastic strands, terminal structures. Heteroneme nematocysts (stenoteles in C,E,F,G and mastigophores in H,I) are only depicted for some species. A - *Erenna laciniiata*, 10x. B - *Lychnagalma utricularia*, 10x. C - *Agalma elegans*, 10x. D - *Resomia ornicephala*, 10x. E - *Frillagalma vityazi*, 20x. F - *Bargmannia amoena*, 10x. G - *Cordagalma* sp., reproduced from Carré 1968. H - *Lilyopsis fluoracantha*, 20x. I - *Abylopsis tetragona*, 20x.

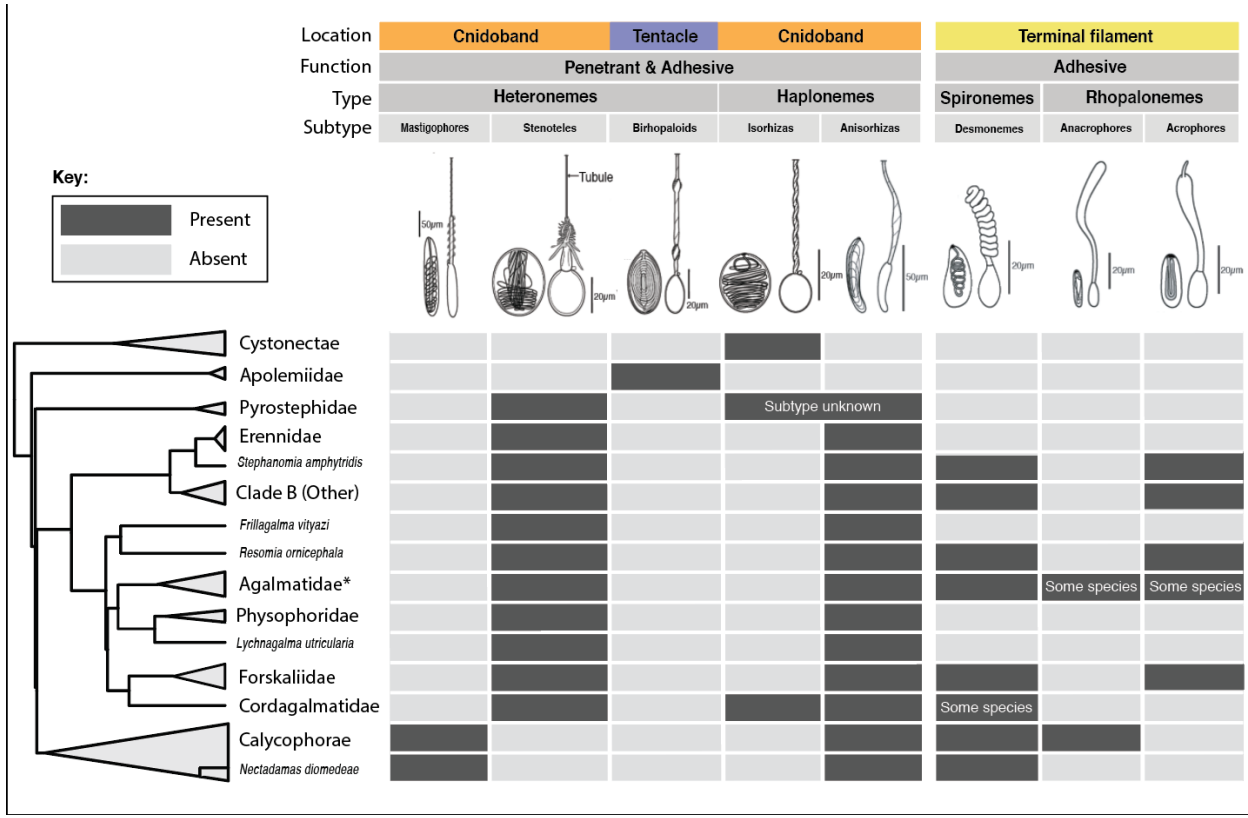


Figure 3: Phylogenetic distribution of nematocyst types, subtypes, functions, and locations in the zooid across the major siphonophore clades. Illustrations reproduced with permission from Mapstone 2014. Undischarged capsules to the left, discharged to the right. Agalmatidae* here refers only to the genera *Agalma*, *Athorybia*, *Halistemma*, and *Nanomia*.

65 work by adhering to the surface of the prey. While recent descriptive studies have expanded
 66 and confirmed our understanding of this diversity, the evolutionary history of nematocyst type
 67 gain and loss in siphonophores remains unexplored. Thus, here we reconstruct the evolution
 68 of shifts, gains, and losses of nematocyst types, subtypes, and other major categorical traits
 69 that led to the extant diversity we see in siphonophore tentilla.

70 Distantly related organisms that evolved to feed on similar resources often evolve similar
 71 adaptations (17). In (14), we found strong associations between piscivory and haploneme
 72 shape across distantly related siphonophore lineages. These associations could have been
 73 produced by convergent changes in the adaptive optima of these characters. Here we
 74 set out to test this hypothesis using comparative model fitting methods. Analyzing the
 75 diversity of morphological states from a phylogenetic perspective allows us to identify the

76 specific evolutionary processes that gave rise to it. Here we fit and compare a variety of
77 macroevolutionary models to siphonophore tentilla morphology measurement data to identify
78 instances of neutral divergence, stabilizing selection, changes in the speed of evolution,
79 convergent evolution, and paedomorphosis (larval characters present in mature colonies).

80 In (14) we fit discriminant analyses to identify characters that are predictive of feeding guild.
81 These discriminant analyses can be used to generate hypotheses on the diets of ecologically
82 understudied siphonophore species for which we have morphology data. Here we present a
83 Bayesian prediction for the feeding guild of 45 species using the morphological dataset in (14).
84 As mentioned above, tentilla are far from being ornamental shapes and are in fact violently
85 reactive weapons for prey capture (14, 18). While we now have detailed characterizations of
86 tentilla morphologies across many species, the diversity of dynamic performances and their
87 relationships to the undischarged morphologies have not been examined to date. To address
88 this gap, we set out to record high-speed video of the *in vivo* discharge dynamics of several
89 siphonophore species at sea, and compare the kinematic attributes to their morphological
90 characters.

91 Methods

92 All character data and the phylogeny analyzed here were published in (14). We log transformed
93 all the continuous characters that did not pass Shapiro-Wilks normality tests, and used
94 the ultrametric constrained Bayesian time tree in all comparative analyses. When missing
95 data was incorporated as inapplicable states, we removed those species with characters that
96 could not be measured due to technical limitations. We used the feeding guild categories
97 detailed in (14) with one modification: including all *Forskalia* spp. as generalists not only
98 a single *Forskalia* species on the tree after a reinterpretation of the data in (19). In order
99 to characterize the evolutionary history of tentilla morphology, we fitted different models
100 generating the observed data distribution given the phylogeny for each continuous character
101 using the function `fitContinuous` in the R package *geiger* (20). These models include a

102 non-phylogenetic white-noise model (WN), a neutral divergence Brownian Motion model
103 (BM), an early-burst decreasing rate model (EB), and an Ornstein-Uhlenbeck (OU) model
104 with stabilizing selection around a fitted optimum trait value. In the same way as (14) we
105 then ordered the models by increasing parametric complexity (WN, BM, EB, OU), and
106 compared their corrected Akaike Information Criterion (AICc) scores (21). We used the
107 lowest (best) score using a delta cutoff of 2 units to determine significance relative to the
108 next simplest model (SM10). We calculated model adequacy scores using the R package
109 *arbutus* (22) (SM11). We calculated phylogenetic signals in each of the measured characters
110 using Blomberg's K (23) (SM10). To reconstruct the ancestral character states of nematocyst
111 types and other categorical traits, we use stochastic character mapping (SIMMAP) using the
112 package *phytools* (24).

113 In order to examine the phenotypic integration in the tentillum, we explored the correla-
114 tional structure among continuous characters and among their evolutionary histories using
115 principal component analysis (PCA) and phylogenetic PCA (24). Since the character dataset
116 contains many gaps due to missing characters and inapplicable states, we carried out these
117 analyses on a subset of species and characters that allowed for the most complete dataset.
118 This was done by removing the terminal filament characters (which are only shared by a small
119 subset of species), and then removing species which had inapplicable states for the remaining
120 characters (apolemiids and cystonects). In addition, we obtained the correlations between
121 the phylogenetic independent contrasts (25) using the package *rphylip* (26). We identified
122 four hypothetical modules among the tentillum characters: (1) The tentillum scaffold module
123 – cnidoband length & width, nematocyst row number, pedicle & elastic strand width, tentacle
124 width; (2) the heteroneme module – heteroneme length & width, shafts length & width; (3)
125 the haploneme module – length and width; and (4) the terminal filament module – desmoneme
126 & rhopaloneme length & width. To test and quantify phenotypic integration between these
127 multivariate modules, we used the phylogenetic phenotypic integration test in the package
128 *geomorph* (27).

When looking at the morphospace of species in different feeding guilds, we also used PCA on the complete tentacular character dataset transforming inapplicable states of absent characters to zeros to account for similarity based on character presence/absence. Using these principal components, we examined the occupation of the morphospace across species in different feeding guilds using a phylogenetic MANOVA with the package *geiger* (20) to assess the variation explained, and a morphological disparity test with the package *geomorph* (27) to assess differences in the extent occupied by each guild.

In order to detect and evaluate instances of convergent evolution, we used the package SURFACE (28). This tool identifies OU regimes and their optima given a tree and character data, and then evaluates where the same regime has appeared independently in different lineages. We applied these analyses to the haploneme nematocyst length and width characters as well as to the most complete dataset without inapplicable character states.

In order to generate hypotheses on the diets of siphonophores using tentilla morphology, we used the discriminant analyses of principal components (DAPC) (29) trained in (14) to predict the feeding guilds of species in the dataset for which there are no published feeding observations.

In order to observe the discharge behavior of different tentilla, we recorded high speed footage (1000-3000 fps) of tentillum and nematocyst discharge by live siphonophore specimens (26 species) using a Phantom Miro 320S camera mounted on a stereoscopic microscope. We mechanically elicited tentillum and nematocyst discharge using a fine metallic pin. We used the Phantom PCC software to analyze the footage. For the 10 species recorded, we measured total cnidoband discharge time (ms), heteroneme filament length (μm), and discharge speeds (mm/s) for cnidoband, heteronemes, haplonemes, and heteroneme shafts when possible (data available in the Dryad repository).

153 **Results**

154 *Evolutionary history of tentillum morphology* – In (14), we produced the most speciose
155 siphonophore molecular phylogeny to date, while incorporating the most recent findings
156 in siphonophore deep node relationships. This phylogeny revealed for the first time that
157 the genus *Erenna* is the sister to *Stephanomia amphytridis*. *Erenna* and *Stephanomia* bear
158 the largest tentilla among all siphonophores, thus their monophyly indicates that there was
159 a single evolutionary transition to giant tentilla. Siphonophore tentilla range in size from
160 ~30 µm in some *Cordagalma* specimens to 2-4 cm in *Erenna* species, and up to 8 cm in
161 *Stephanomia amphytridis* (10). Most siphonophore tentilla measure between 175 and 1007
162 µm (1st and 3rd quartiles), with a median of 373 µm. The extreme gain of tentillum size in
163 this newly found clade may have important implications for access to large prey size classes
164 such as adult deep-sea fishes.

165 Siphonophore tentilla are defined as lateral, monostichous evaginations of the tentacle
166 (including its gastrovascular lumen), armed with epidermal nematocysts (11). The buttons on
167 *Physalia* tentacles were not traditionally regarded as tentilla, but (8) and our observations (13),
168 confirm that the buttons contain evaginations of the gastrovascular lumen, thus satisfying all
169 the criteria for the definition. In this light, and given that most Cystonectae bear conspicuous
170 tentilla, we conclude (in agreement with (13) and (14)) that tentilla were present in the most
171 recent common ancestor of all siphonophores, and secondarily lost twice, once in *Apolemia* and
172 again in *Bathyphysa conifera*. In order to gain a broad perspective on the evolutionary history
173 of tentilla, we reconstructed the phylogenetic positions of the main categorical character
174 shifts using stochastic character mapping (SM1-9) and summarized in (Fig. 4). Some of
175 these characters include the gain and loss of nematocyst types.

176 We assume that haploneme nematocysts are ancestrally present in siphonophore tentacles
177 since they are present in the tentacles of many other hydrozoans (15). Haplonemes are
178 toxin-bearing open-ended nematocysts characterized by the lack of a shaft preceding the
179 tubule. Two subtypes are found in siphonophores: the isorhizas of homogeneous tubule

width, and the anisorhizas with a slight bulking of the tubule near the base. In Cystonectae, haplonemes diverged into spherical isorhizas of two size classes. There is one size of haplonemes in Codonophora, which consist of elongated anisorhizas. Haplonemes were likely lost in the tentacles of *Apolemia* but retained as spherical isorhizas in other *Apolemia* tissues (30). While heteronemes exist in other tissues of cystonects, they appear in the tentacles of codonophorans exclusively, as birhopaloids in *Apolemia*, stenoteles in eucladophoran physonects, and microbasic mastigophores in calycophorans. The four nematocyst types unique to siphonophores appear in two events in the phylogeny (Fig. 4): birhopaloids arose in the stem to *Apolemia*, while rhopalonemes (acrophore and anacrophore) and homotrichous anisorhizas arose in the stem to Tendiculophora.

Nematocyst type gain and loss is also associated with prey capture functions. For example, the loss of desmonemes and rhopalonemes in piscivorous *Erenna*, retaining solely the penetrant (and venom injecting) anisothizas and stenoteles (two size classes) is reminiscent of the two size classes of penetrant isorhizas in the fish-specialist cystonects. Moreover, with the gain of anisorhizas, desmonemes, and rhopalonemes, the Tendiculophora gained versatility in entangling and adhesive functions of the cnidoband and terminal filament, which may have allowed their feeding niches to diversify. Part of the effectiveness of calycophoran cnidobands at entangling crustaceans may be attributed to the subspecialization of their heteronemes. These shifted from the ancestral penetrating stenotele to the microbasic mastigophore (or eurytele in some species) with a long barmed shaft with many long spines. This heteroneme subtype could be better at interlocking with the setae of crustacean legs and antennae.

In those species that have a functional terminal filament, the desmonemes and rhopalonemes play a fundamental role in the first stages of adhesion of the prey. In many species, the tugs of the struggling prey on the terminal filament trigger the cnidoband discharge (18). The adhesive terminal filament has been lost several times in the Euphysonectae (*Frillagalma*, *Lychnagalma-Physophora*, *Erenna*, and some species of *Cordagalma*). In these species, we hypothesize that a different trigger mechanism is at play, possibly involving the

207 prey actively biting or grasping the tentillum or lure.

208 The clades defined in (14) are characterized by unique evolutionary innovations in their
209 tentilla. The clade Eucladophora (containing Pyrostephidae, Euphysonectae, and Caly-
210 cophorae) encompasses all of the extant Siphonophore species (178 of 186) except Cystonects
211 and *Apolemia*. Innovations that arose along the stem of this group include spatially seg-
212 regated heteroneme and haploneme nematocysts, terminal filaments, and elastic strands
213 (Fig. 4). Pyrostephids evolved a unique bifurcation of the axial gastrovascular canal of
214 the tentillum known as the “saccus” (11). The stem to the clade Tendiculophora (clade
215 containing Euphysonectae and Calycophorae) subsequently acquired further novelties such
216 as the desmoneme and rhopaloneme (acrophore subtype ancestral) nematocysts on the
217 terminal filament (Fig. 4), which bears no other nematocyst type. These are arranged
218 in sets of 2 parallel rhopalonemes for each single desmoneme (31, 32). The involucrum is
219 an expansion of the epidermal layer that can cover part or all of the cnidoband (Fig. 2).
220 This structure, together with differentiated larval tentilla, appeared in the stem branch to
221 Clade A physonects. Calycophorans evolved novelties such as larger desmonemes at the
222 distal end of the cnidoband, pleated pedicles with a “hood” (here considered homologous
223 to the involucrum) at the proximal end of the tentillum, anacrophore rhopalonemes, and
224 microbasic mastigophore-type heteronemes. While calycophorans have diversified into most
225 of the extant described siphonophore species (108 of 186), their tentilla have not undergone
226 any major categorical gains or losses since their most recent common ancestor. Nonetheless,
227 they have evolved a wide variation in nematocyst and cnidoband sizes. Ancestrally (and
228 retained in most prayomorphs and hippopodids), the calycophoran tentillum is recurved
229 where the proximal and distal ends of the cnidoband are close together. Diphyomorph tentilla
230 are slightly different in shape, with straighter cnidobands.

231 *Evolution of tentillum and nematocyst characters* – Most (74%) characters present a
232 significant phylogenetic signal, yet only total nematocyst volume, haploneme length, and
233 heteroneme-to-cnidoband length ratio had a phylogenetic signal with K larger than 1. Total

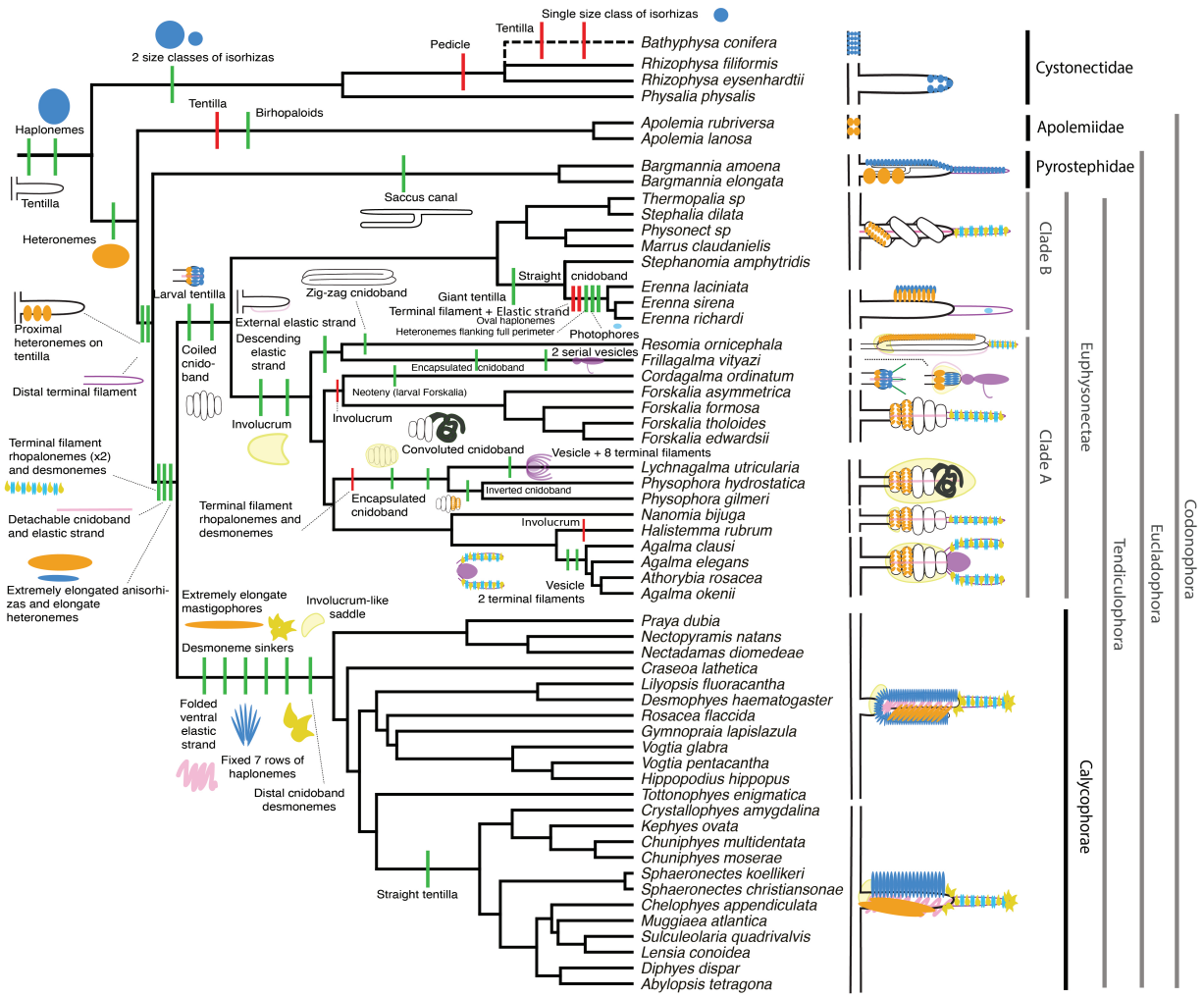


Figure 4: Siphonophore cladogram with the main categorical character gains (green) and losses (red) mapped. Some branch lengths were modified from the Bayesian chronogram to improve readability. The main visually distinguishable tentillum types are sketched next to the species that bear them, showing the location and arrangement of the main characters. In large, complex-shaped euphysonect tentilla, haplonemes were omitted for simplification. The hypothesized phylogenetic placement of the rhizophysid *Bathyphysa conifera*, for which no molecular data are yet available, was added manually (dashed line).

²³⁴ nematocyst volume and cnidoband-to-heteroneme length ratio showed strongly conserved
²³⁵ phylogenetic signals. The majority (67%) of characters were best fitted by BM models,
²³⁶ indicating a history of neutral constant divergence. We did not find any relationship
²³⁷ between phylogenetic signal and specific model support, where characters with high and low
²³⁸ phylogenetic signal were broadly distributed among the best fitted for each model. One-
²³⁹ third of the characters measured in (14) did not recover significant support for any of the
²⁴⁰ phylogenetic models tested, indicating they are either not phylogenetically conserved, or
²⁴¹ they evolved under a complex evolutionary process not represented among the models tested
²⁴² (SM10). Haploneme nematocyst length was the only character with support for an EB model
²⁴³ of decreasing rate of evolution with time. No character had support for a single-optimum OU
²⁴⁴ model (when not informed by feeding guild regime priors). The model adequacy tests (SM11)
²⁴⁵ indicate that many characters may have a relationship between the states and the rates of
²⁴⁶ evolution (Sasr) not captured in the basic models compared here, accompanied by a signal
²⁴⁷ of unaccounted rate heterogeneity (Cvar). No characters show significant deviations in the
²⁴⁸ overall rate of evolution estimated (Msig). Some characters show a perfect fit (no significant
²⁴⁹ deviations across all metrics) under BM evolution, such as heteroneme shape, length, width
²⁵⁰ & volume, haploneme width & SA/V, tentacle width and pedicle width. Haploneme row
²⁵¹ number and rhopaloneme shape have significant deviations across four metrics, indicating
²⁵² that BM (best model) is a poor fit. These characters likely evolved under complex models
²⁵³ which would require many more data points than we have available to fit with accuracy.

²⁵⁴ *Evolution of nematocyst shape* – The greatest evolutionary change in haploneme nema-
²⁵⁵ tocyst shape occurred in a single shift towards elongation in the stem of Tendiculophora,
²⁵⁶ which contains the majority of described siphonophore species, *i.e.* all siphonophores other
²⁵⁷ than Cystonects, *Apolemia*, and Pyrostephidae. There is one secondary return to more
²⁵⁸ oval, less elongated haplonemes in *Erenna*, but it does not reach the sphericity present
²⁵⁹ in Cystonectae or Pyrostephidae (Fig. 6). Heteroneme evolution presents a less discrete
²⁶⁰ evolutionary history. Tendiculophora evolved more elongate heteronemes along the stem, but

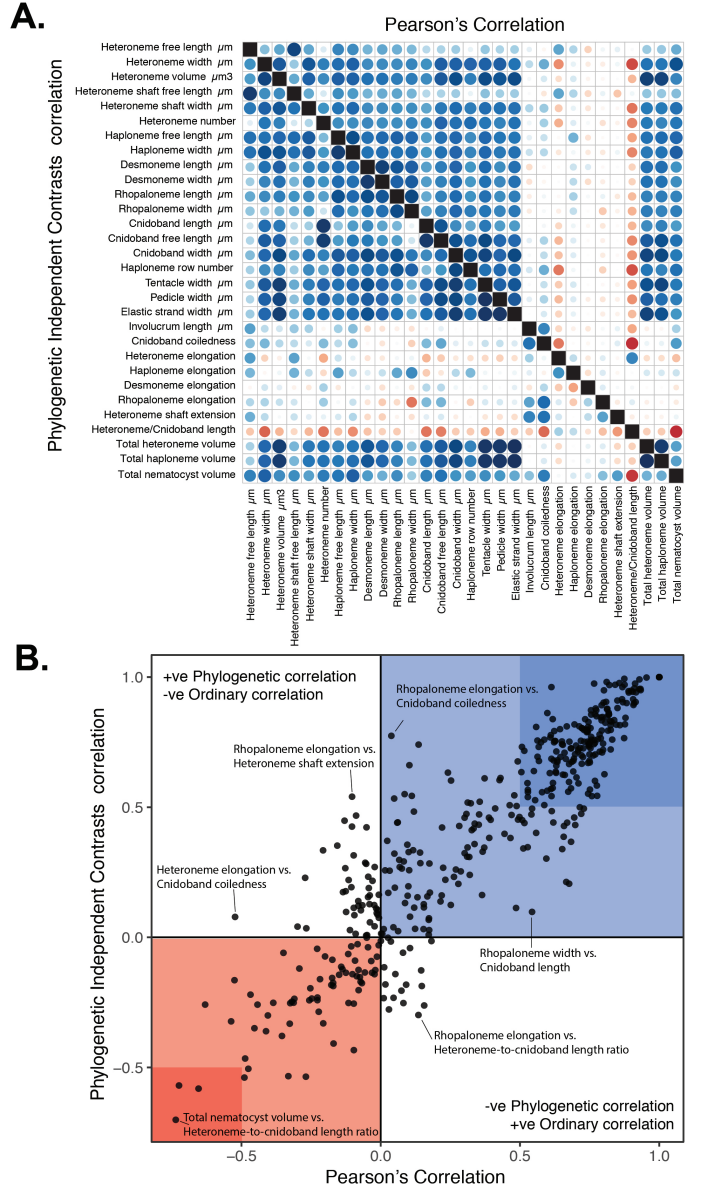


Figure 5: A. Correlogram showing strength of ordinary (upper triangle) and phylogenetic (lower triangle) correlations between characters. Both size and color of the circles indicate the strength of the correlation (R^2). B. Scatterplot of phylogenetic correlation against ordinary correlation showing a strong linear relationship ($R^2 = 0.92$, 95% confidence between 0.90 and 0.93). Light red and blue boxes indicate congruent negative and positive correlations respectively. Darker red and blue boxes indicate strong (<-0.5 or >0.5) negative and positive correlation coefficients respectively.

261 the difference between theirs and other siphonophores' is much smaller than the variation
262 in shape within Tendiculophora, bearing no phylogenetic signal within this clade. In this
263 clade, the evolution of heteroneme shape has diverged in both directions, and there is no
264 correlation with haploneme shape (Fig. 6), which has remained fairly constant (elongation
265 between 1.5 and 2.5).

266 Haploneme and heteroneme shape share 21% of their variance across extant values, and
267 53% of the variance in their shifts along the branches of the phylogeny. However, much of
268 this correlation is due to the sharp contrast between Pyrostephidae and their sister group
269 Tendiculophora. We searched for regime shifts in the evolution of haploneme nematocyst
270 shape characters using SURFACE (28). SURFACE identified eight distinct OU regimes in
271 the evolutionary history of haploneme length and width (Fig. 9A). The different regimes are
272 located (1) in cystonects, (2) in most of Tendiculophora, (3) in most diphyomorphs, (4) in
273 *Cordagalma ordinatum*, (5) in *Stephanomia amphytridis*, (6) in pyrostephids, (7) in *Diphyes*
274 *dispar* + *Abylopsis tetragona*, and (8) in *Erenna* spp.

275 *Phenotypic integration of the tentillum* – Phenotypically integrated structures maintain
276 evolutionary correlations between its constituent characters. Of the phylogenetic correlations
277 (Fig. 5a, lower triangle), 81.3% were positive and 18.7% were negative, while of the ordinary
278 correlations (Fig. 5a, upper triangle) 74.6% were positive and 25.4% were negative. Half
279 (49.9%) of phylogenetic correlations were >0.5 , while only 3.6% are < -0.5 . Similarly, among
280 the correlations across extant species, 49.1% were >0.5 and only 1.5% were < -0.5 . In
281 addition, we found that 13.9% of character pairs had opposing phylogenetic and ordinary
282 correlation coefficients. Just 4% have negative phylogenetic and positive ordinary correlations
283 (such as rhopaloneme elongation ~ heteroneme-to-cnidoband length ratio and haploneme
284 elongation, or haploneme elongation ~ heteroneme number), and only 9.9% of character pairs
285 had positive phylogenetic correlation yet negative ordinary correlation (such as heteroneme
286 elongation ~ cnidoband convolution and involucrum length, or rhopaloneme elongation with
287 cnidoband length). These disparities could be explained by Simpson's paradox (33): the

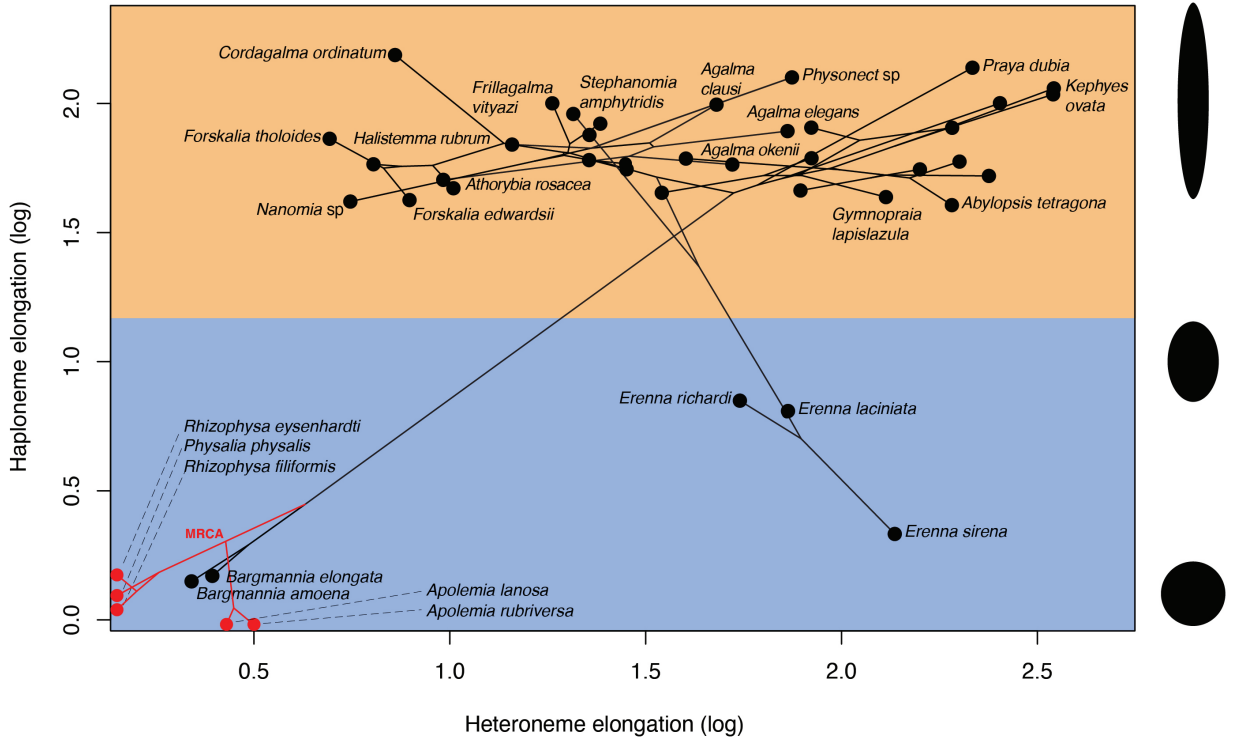


Figure 6: Phylomorphospace showing haploneme and heteroneme elongation (log scaled). Orange area delimits rod-shaped haplonemes, the blue area covers oval and round-shaped haplonemes. Smaller dots and lines represent phylogenetic relationships and ancestral states of internal nodes under BM. Species nodes in red lack either haplonemes or heteronemes, and their values are projected onto the axis of the nematocyst type they bear. Cystonects have no tentacle heteronemes and are projected onto the haploneme axis. Apolemiids have no tentacle haplonemes and are projected onto the heteroneme axis.

reversal of the sign of a relationship when a third variable (or a phylogenetic topology (34)) is considered. However, no character pair had correlation coefficient differences larger than 0.64 between ordinary and phylogenetic correlations (heteroneme shaft extension ~ rhopaloneme elongation has a Pearson's correlation of 0.10 and a phylogenetic correlation of -0.54). Rhopaloneme elongation shows the most incongruencies between phylogenetic and ordinary correlations with other characters. The phenotypic integration test showed significant integration signal between all modules, tentillum and haploneme modules sharing the greatest regression coefficient (SM12).

In the non-phylogenetic PCA morphospace using only characters derived from simple measurements (Fig. 7), PC1 (aligned with tentillum and tentacle size) explained 69.3% of the variation in the tentillum morphospace, whereas PC2 (aligned with heteroneme length, heteroneme number, and haploneme arrangement) explained 13.5%. In a phylogenetic PCA, 63% of the evolutionary variation in the morphospace is explained by PC1 (aligned with shifts in tentillum size), while 18% is explained by PC2 (aligned with shifts in heteroneme number and involucrum length).

Morphospace occupation – In order to examine the occupation structure of the morphospace across all siphonophore species in the dataset, we cast a PCA on the data after transforming inapplicable states (due to absence of character) to zeroes. This allows us to accommodate species with many missing characters (such as cystonects or apolemiids), and to account for common absences as morphological similarities. In this ordination, PC1 (aligned with cnidoband size) explains 47.45% of variation and PC2 (aligned with heteroneme volume and involucrum length) explains 16.73% of variation . When superimposing feeding guilds onto the morphospace (Fig. 8), we find that the morphospaces of each feeding guild are only slightly overlapping in PC1 and PC2. A phylogenetic MANOVA showed that feeding guilds explain 27.63% of variance across extant species (p value < 0.000001), and 20.97% of the variance in the tree species accounting for phylogeny, an outcome significantly distinct from the expectation under neutral evolution (p -value = 0.0196). In addition, a morphological

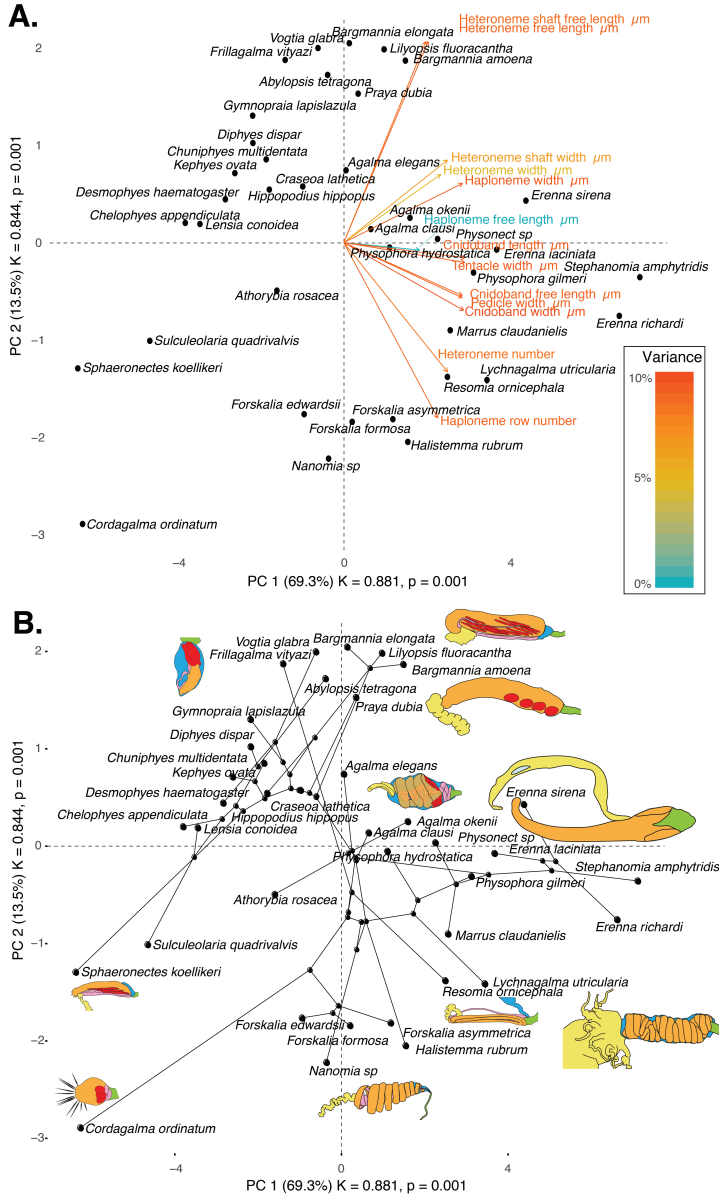


Figure 7: Phylomorphospace of the simple-measurement continuous characters principal components, excluding ratios and composite characters. A. Variance explained by each variable in the PC1-PC2 plane. Axis labels include the phylogenetic signal (K) for each component and p-value. B. Phylogenetic relationships between the species points distributed in that same space.

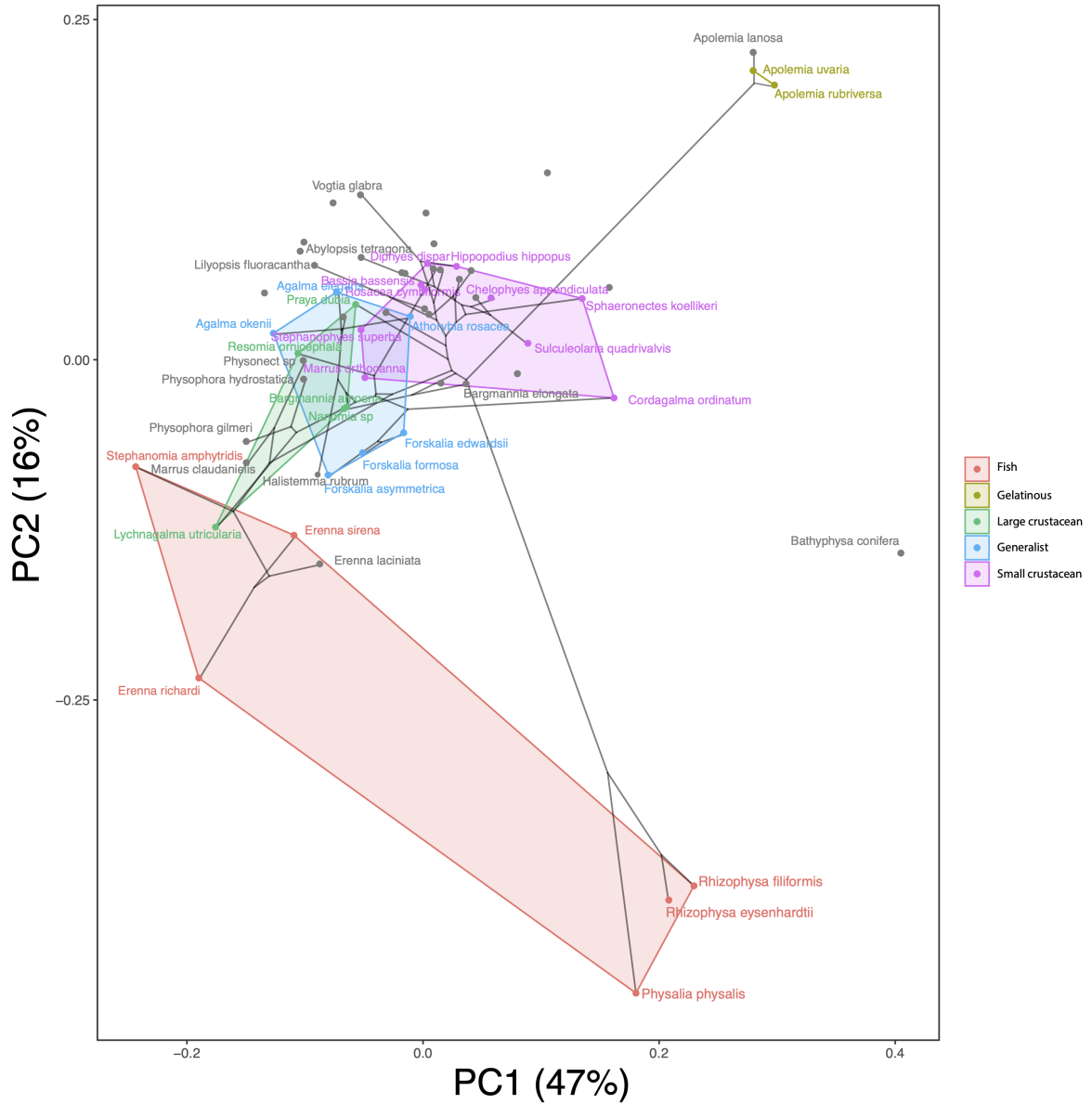


Figure 8: Phylomorphospace showing PC1 and PC2 from a PCA of continuous morphological characters with inapplicable states transformed to zeroes, overlapped with polygons conservatively defining the space occupied by each feeding guild. Lines between species coordinates show the phylogenetic relationships between them.

³¹⁵ disparity analysis accounting for phylogenetic structure shows that the morphospace of fish
³¹⁶ specialists is significantly broader than that of generalists and other specialists. This is due to
³¹⁷ the large morphological disparities between cystonects and piscivorous euphysonects. There
³¹⁸ are no significant differences among the morphospace disparities of the other feeding guilds.

³¹⁹ *Convergent evolution* – Convergence is a widespread evolutionary phenomenon where
³²⁰ distantly related clades independently evolve similar phenotypes. When the dimensionality of
³²¹ the state space is small as it is in tentilla morphology, convergence is more likely given the same
³²² amount of evolutionary change. Using the package SURFACE (28), we identified convergence
³²³ in haploneme nematocyst shape and in morphospace position. In (14), we identified haploneme
³²⁴ nematocyst shape as one of the traits associated with the convergent evolution of piscivory.
³²⁵ Here we find that indeed wider haploneme nematocysts have convergently evolved in the
³²⁶ piscivore cytonects and *Erenna* spp. (Fig. 9A). Extremely narrow haplonemes have also
³²⁷ evolved convergently in *Cordagalma ordinatum* and copepod specialist calycophorans such as
³²⁸ *Sphaeronectes koellikeri*. When integrating many traits into a couple principal components, we
³²⁹ find two distinct convergences between euphysonects and calycophorans with a reduced prey
³³⁰ capture apparatus. Those convergences are between *Frillagalma vityazi* and calycophorans,
³³¹ and once again between *Cordagalma ordinatum* and *Sphaeronectes koellikeri* (Fig. 9B).

³³² *Functional morphology of tentillum and nematocyst discharge* – Tentillum and nematocyst
³³³ discharge high speed videos and measurements are available in the Dryad repository. While
³³⁴ the sample sizes of these measurements were insufficient to draw reliable statistical results
³³⁵ at a phylogenetic level, we did observe patterns that may be relevant to their functional
³³⁶ morphology. For example, cnidoband length is strongly correlated with discharge speed (p
³³⁷ value = 0.0002). This explains much of the considerable difference between euphysonect and
³³⁸ calycophoran tentilla discharge speeds (average discharge speeds: 225.0mm/s and 41.8mm/s
³³⁹ respectively; t-test p value = 0.011), since the euphysonects have larger tentilla than the
³⁴⁰ calycophorans among the species recorded. In addition, we observed that calycophoran
³⁴¹ haploneme tubules fire faster than those of euphysonects (t-test p value = 0.001). Haploneme

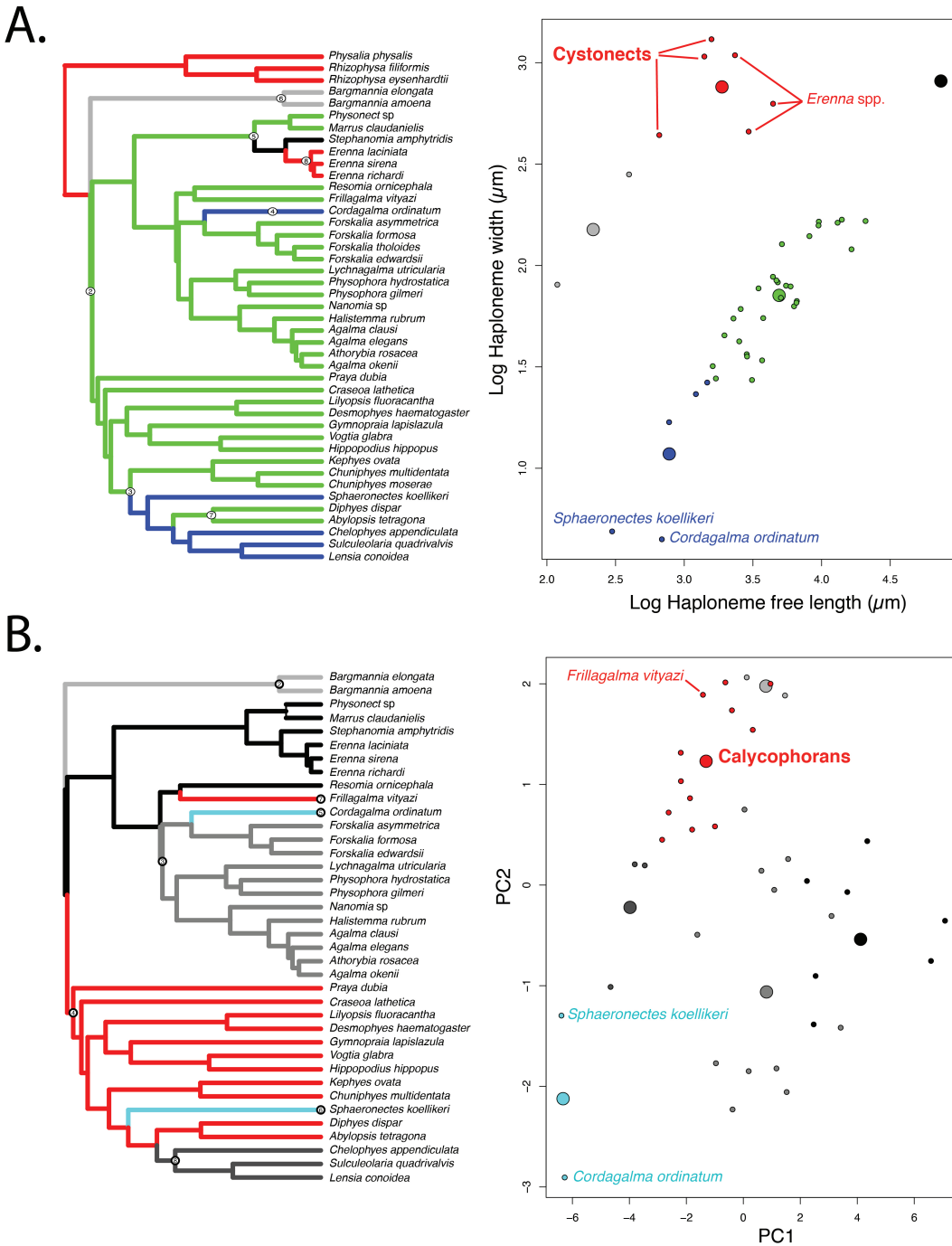


Figure 9: SURFACE plots showing convergent evolutionary regimes modelled under OU for (A) haploneme nematocyst length & width, and (B) for PC1 & 2 of all continuous characters with the exception of terminal filament nematocysts, and removing taxa with inapplicable character states. Node numbers on the tree label different regimes, regimes of the same color are identified as convergent. Small circles on the scatterplots indicate species values, large circles indicate the average position of the OU optima (θ) for a given combination of convergent regimes.

³⁴² nematocysts discharge 2.8x faster than heteroneme nematocysts (t-test p value = 0.0012).

³⁴³ Finally, we observed that the stenoteles of the Euphysonectae discharge a helical filament

³⁴⁴ that “drills” itself through the medium it penetrates as it everts.

³⁴⁵ *Generating dietary hypotheses using tentillum morphology* – For many siphonophore species,
³⁴⁶ no feeding observations have yet been published. To help bridge this gap of knowledge,
³⁴⁷ we generated hypotheses about the diets of these understudied siphonophores based on
³⁴⁸ their known tentacle morphology using one of the linear discriminant analyses of principal
³⁴⁹ components (DAPC) fitted in (14). This provides concrete predictions to be tested in
³⁵⁰ future work and helps extrapolate our findings to many poorly known species that are
³⁵¹ extremely difficult to collect and observe. The discriminant analysis for feeding guild (7
³⁵² principal components, 4 discriminants) produced 100% discrimination, and the highest loading
³⁵³ contributions were found for the characters (ordered from highest to lowest): Involutrum
³⁵⁴ length, heteroneme volume, heteroneme number, total heteroneme volume, tentacle width,
³⁵⁵ heteroneme length, total nematocyst volume, and heteroneme width. We used the predictions
³⁵⁶ from this discriminant function to generate hypotheses about the feeding guild of 45 species
³⁵⁷ in the morphological dataset. This extrapolation predicts that two other *Apolemia* species are
³⁵⁸ gelatinous prey specialists like *Apolemia rubriversa*, and predicts that *Erenna laciniata* is a
³⁵⁹ fish specialist like *Erenna richardi*. When predicting soft- and hard-bodied prey specialization,
³⁶⁰ the DAPC achieved 90.9% discrimination success, only marginally confounding hard-bodied
³⁶¹ specialists with generalists (SM13). The main characters driving this discrimination are
³⁶² involutrum length, heteroneme number, heteroneme volume, tentacle width, total nematocyst
³⁶³ volume, total haploneme volume, elastic strand width, and heteroneme length.

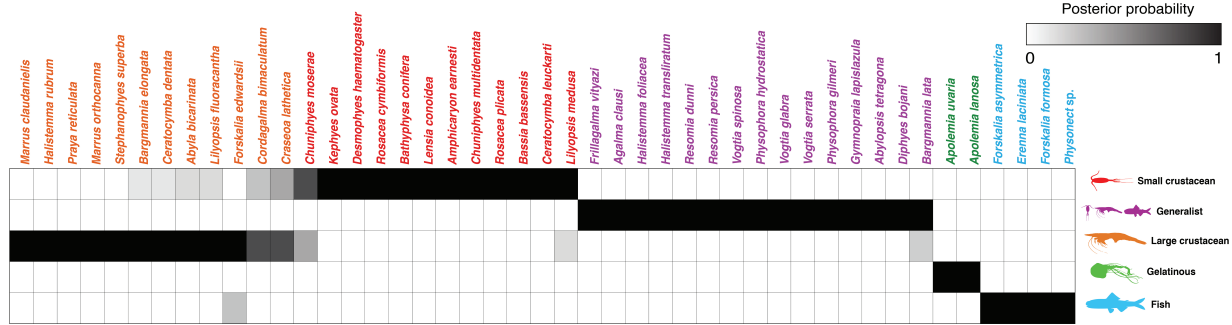


Figure 10: Hypothetical feeding guilds for siphonophore species predicted by a 6 PCA DAPC. Cell darkness indicates the posterior probability of belonging to each guild. Training data set transformed so inapplicable states are computed as zeroes. Species ordered and colored according to their predicted feeding guild.

364 Discussion

365 *On the evolution of tentilla morphology* – Siphonophore tentilla are beautifully complex and
 366 highly diverse. Our new analyses show, however, that the siphonophore tentillum morphospace
 367 actually has a fairly low extant dimensionality due to having an evolutionary history with
 368 many synchronous, correlated changes. This can be due to many causes including structural
 369 constraints, shared developmental programs (by homology or proximity), or natural selection
 370 on separate developmental programs to preserve an adaptive function. Most tentillum
 371 characters develop from a common bud (budding tentilla near the base of the tentacle),
 372 and different nematocyst subtypes share a common evolutionary and developmental origin
 373 (35, 36). In this sense, correlations within these modules are expected for reasons other
 374 than adaptive natural selection. However, we also found correlations between nematocyst
 375 and tentillum characters. Siphonophore tentacle nematocysts (in their cnidocytes) are not
 376 produced nor matured in the developing tentillum. These cnidocytes are produced by
 377 dividing cnidoblasts in the basigaster (basal swelling of the gastrozooid). Once the cnidocytes
 378 have assembled the nematocyst, they migrate outward along the tentacle (37) and position
 379 themselves in the tentillum according to their type and size (31). Thus, the developmental
 380 programs that produce the observed nematocyst morphologies are spatially separated from
 381 those producing the tentillum morphologies, and they originate from evolutionarily distinct

382 cell lineages. Therefore, we hypothesize the genetic correlations and phenotypic integration
383 between tentillum and nematocyst characters are maintained through natural selection on
384 separate regulatory networks, out of the necessity to work together and meet the spatial,
385 mechanical, and functional constraints of their prey capture behavior. In order to adequately
386 test these hypotheses, future work would need to study the genetic mechanisms underlying
387 the development of tentilla from a comparative, evolutionary approach. Fortunately, the
388 unique biology of siphonophore tentacles displays the full developmental sequence of tentilla
389 along each tentacle, making siphonophores an ideal system for the comparative study of
390 development.

391 The evolutionary rate covariance results in (14) indicated that tentilla are not only
392 phenotypically integrated (with widespread evolutionary correlations across structures) but
393 also show patterns of evolutionary modularity, where different sets of characters appear
394 to evolve in stronger correlations among each other than with other characters (38). This
395 may be indicative of the underlying genetic and developmental dependencies among closely
396 homologous nematocyst types (such as desmonemes and rhopalonemes) and structures. The
397 rate covariance results are congruent with the evolutionary correlations we found (Fig. 5). In
398 addition, these evolutionary modules point to hypothetical functional modules. For example,
399 the coiling degree of the cnidoband and the extent of the involucrum have correlated rates
400 of evolution, while high-speed videos show that the involucrum helps direct the whiplash
401 of the uncoiling cnidoband distally (towards the prey). The evolutionary innovation of the
402 Tendiculophora tentilla with shooting cnidobands and modular regions may have facilitated
403 further dietary diversification. A specific instance of this may have been the access to the
404 abundant small crustacean prey such as copepods. The rapid darting escape response of
405 copepods may preclude their capture in siphonophores without shooting cnidobands. Dietary
406 diversification may be related to the far greater number of species in Tendicilophora than its
407 relatives Cystonectae, Apolemiidae, and Pyrostephidae.

408 *Heterochrony and convergence in the evolution of tentilla with diet* - In addition to

409 identifying shifts in prey type, (14) revealed the specific morphological changes in the prey
410 capture apparatus associated with these changes. Copepod-specialized diets have evolved
411 independently in *Cordagalma* and some calycophorans. These evolutionary transitions
412 happened together with transitions to smaller tentilla with fewer and smaller cnidoband
413 nematocysts. We found that these morphological transitions evolved convergently in these
414 taxa. Tentilla are expensive single-use structures (18), therefore we would expect that
415 specialization in small prey would beget reductions in the size of the prey capture apparatus
416 to the minimum required for the ecological performance. Such a reduction in size would
417 require extremely fast rates of trait evolution in an ordinary scenario. However, *Cordagalma*'s
418 tentilla strongly resemble the larval tentilla (only found in the first-budded feeding body of
419 the colony) of their sister genus *Forskalia*. This indicates that the evolution of *Cordagalma*
420 tentilla could be a case of paedomorphic heterochrony associated with predatory specialization
421 on smaller prey. This developmental shift may have provided a shortcut for the evolution of
422 a smaller prey capture apparatus.

423 Our work identifies yet another novel example of convergent evolution. The region of the
424 tentillum morphospace (Fig. 7 & Fig. 9B) occupied by calycophorans was independently (and
425 more recently) occupied by the physonect *Frillagalma vityazi*. Like calycophorans, *Frillagalma*
426 tentilla have small C-shaped cnidobands with a few rows of anisorhizas. Unlike calycophorans,
427 they lack paired elongate microbasic mastigophores. Instead, they bear exactly three oval
428 stenoteles, and their cnidobands are followed by a branched vesicle, unique to this genus.
429 Their tentillum morphology is very different from that of other related physonects, which tend
430 to have long, coiled, cnidobands with many paired oval stenoteles. Our SURFACE analysis
431 clearly indicates a regime convergence in the cnidoband morphospace between *Frillagalma*
432 and calycophorans (Fig. 9B). Most studies on calycophoran diets have reported their prey to
433 be primarily composed of small crustaceans, such as copepods or ostracods (19, 39). The
434 diet of *Frillagalma vityazi* is unknown, but this morphological convergence suggests that they
435 evolved to capture similar kinds of prey. The DAPCs in (14) predict that *Frillagalma* has a

436 generalist niche with both soft and hard-bodied prey, including copepods.

437 *Evolution of nematocyst shape* – A remarkable feature of siphonophore haplonemes is
438 that they are outliers to all other Medusozoa in their surface area to volume relationships,
439 deviating significantly from sphericity (40). This suggests a different mechanism for their
440 discharge that could be more reliant on capsule tension than on osmotic potentials (41), and
441 strong selection for efficient nematocyst packing in the cnidoband (31, 40). Our results show
442 that Codonophora underwent a shift towards elongation and Cystonectae towards sphericity,
443 assuming the common ancestor had an intermediate state. Since we know that the haplonemes
444 of other hydrozoan outgroups are generally spheroid, it is more parsimonious to assume that
445 cystonects are simply retaining this ancestral state. Later, we observe a return to more
446 rounded (ancestral) haplonemes in *Erenna*, concurrent with a secondary gain of a piscivorous
447 trophic niche, like that exhibited by cystonects. Our SURFACE analysis shows that this
448 transition to roundness is convergent with the regime occupied by cystonects (Fig. 9A).
449 Purcell (39) showed that haplonemes have a penetrating function as isorhizas in cystonects
450 and an adhesive function as anisorhizas in Tendiculophora. It is no coincidence that the two
451 clades that have converged to feed primarily on fish have also converged morphologically
452 toward more compact haplonemes. Isorhizas in cystonects are known to penetrate the skin of
453 fish during prey capture, and to deliver the toxins that aid in paralysis and digestion (42).
454 *Erenna*'s anisorhizas are also able to penetrate human skin and deliver a painful sting (4)
455 (and pers. obs.), a common feature of piscivorous cnidarians like the Portuguese man-o-war
456 or box jellies.

457 The implications of these results for the evolution of nematocyst function are that an
458 innovation in the discharge mechanism of haplonemes may have occurred during the main shift
459 to elongation. Elongate nematocysts can be tightly packed into cnidobands. We hypothesize
460 this may be a Tendiculophora lineage-specific adaptation to packing more nematocysts into a
461 limited tentillum space, as suggested by (31). Thomason (40) hypothesized that smaller, more
462 spherical nematocysts, with a lower surface area to volume ratio, are more efficient in osmotic-

463 driven discharge and thus have more power for skin penetration. The elongated haplonemes
464 of crustacean-eating Tendiculophora have never been observed penetrating their crustacean
465 prey (39), and are hypothesized to entangle the prey through adhesion of the abundant
466 spines to the exoskeletal surfaces and appendages. Entangling requires less acceleration and
467 power during discharge than penetration, as it does not rely on point pressure. In fish-eating
468 cystonects and *Erenna* species, the haplonemes are much less elongated and very effective at
469 penetration, in congruence with the osmotic discharge hypothesis. Tendiculophora, composed
470 of the clades Euphysonectae and Calycophorae, includes the majority of siphonophore species.
471 Within these clades are the most abundant siphonophore species, and a greater morphological
472 and ecological diversity is found. We hypothesize that this packing-efficient haploneme
473 morphology may have also been a key innovation leading to the diversification of this clade.
474 However, other characters that shifted concurrently in the stem of this clade could have been
475 equally responsible for their extant diversity.

476 *Generating hypotheses on siphonophore feeding ecology* – One motivation for our research
477 is to understand the links between prey-capture tools and diets so we can generate hypotheses
478 about the diets of predators based on morphological characteristics. Indeed, our discriminant
479 analyses were able to distinguish between different siphonophore diets based on morphological
480 characters alone. The models produced by these analyses generated testable predictions
481 about the diets of many species for which we only have morphological data of their tentacles.
482 While the limited dataset used here is informative for generating tentative hypotheses, the
483 empirical dietary data are still scarce and insufficient to cast robust predictions. This reveals
484 the need to extensively characterize siphonophore diets and feeding habits. In future work, we
485 will test these ecological hypotheses and validate these models by directly characterizing the
486 diets of some of those siphonophore species. Predicting diet using morphology is a powerful
487 tool to reconstruct food web topologies from community composition alone. In many of the
488 ecological models found in the literature, interactions among the oceanic zooplankton have
489 been treated as a black box (43). The ability to predict such interactions, including those of

⁴⁹⁰ siphonophores and their prey, will enhance the taxonomic resolution of nutrient-flow models
⁴⁹¹ constructed from plankton community composition data.

⁴⁹² **Acknowledgements**

⁴⁹³ This work was supported by the Society of Systematic Biologists (Graduate Student Award
⁴⁹⁴ to A.D.S.); the Yale Institute of Biospheric Studies (Doctoral Pilot Grant to A.D.S.); and
⁴⁹⁵ the National Science Foundation (Waterman Award to C.W.D., and NSF-OCE 1829835 to
⁴⁹⁶ C.W.D., S.H.D.H., and C. Anela Choy). A.D.S. was supported by a Fulbright Spain Graduate
⁴⁹⁷ Studies Scholarship.

⁴⁹⁸ **References**

- ⁴⁹⁹ 1. Pugh P (1983) *Benthic siphonophores: A review of the family rhodaliidai (siphonophora, physonectae)* (Royal Society).
- ⁵⁰¹ 2. Pugh P, Harbison G (1986) New observations on a rare physonect siphonophore, lychnagalma utricularia (claus, 1879). *Journal of the Marine Biological Association of the United Kingdom* 66(3):695–710.
- ⁵⁰⁴ 3. Pugh P, Youngbluth M (1988) Two new species of prayine siphonophore (calycophorae, prayidae) collected by the submersibles johnson-sea-link i and ii. *Journal of Plankton Research* 10(4):637–657.
- ⁵⁰⁷ 4. Pugh P (2001) A review of the genus erenna bedot, 1904 (siphonophora, physonectae). *BULLETIN-NATURAL HISTORY MUSEUM ZOOLOGY SERIES* 67(2):169–182.
- ⁵⁰⁹ 5. Hissmann K (2005) In situ observations on benthic siphonophores (physonectae: Rhodaliidae) and descriptions of three new species from indonesia and south africa. *Systematics and Biodiversity* 2(3):223–249.
- ⁵¹² 6. Haddock SH, Dunn CW, Pugh PR (2005) A re-examination of siphonophore terminology and morphology, applied to the description of two new prayine species with remarkable bio-optical properties. *Journal of the Marine Biological Association of the United Kingdom*

- 515 85(3):695–707.
- 516 7. Dunn CW, Pugh PR, Haddock SH (2005) *Marrus claudanielis*, a new species of
517 deep-sea physonect siphonophore (siphonophora, physonectae). *Bulletin of Marine Science*
518 76(3):699–714.
- 519 8. Bardi J, Marques AC (2007) Taxonomic redescription of the portuguese man-of-war,
520 physalia physalis (cnidaria, hydrozoa, siphonophorae, cystonectae) from brazil. *Iheringia*
521 *Série Zoologia* 97(4):425–433.
- 522 9. Pugh P, Haddock S (2010) Three new species of remosiid siphonophore (siphonophora:
523 Physonectae). *Journal of the Marine Biological Association of the United Kingdom* 90(6):1119–
524 1143.
- 525 10. Pugh P, Baxter E (2014) A review of the physonect siphonophore genera halistemma
526 (family agalmatidae) and stephanomia (family stephanomiidae). *Zootaxa* 3897(1):1–111.
- 527 11. Totton AK, Bargmann HE (1965) *A synopsis of the siphonophora* (British Museum
528 (Natural History)).
- 529 12. Mapstone GM (2014) Global diversity and review of siphonophorae (cnidaria: Hydro-
530 zoa). *PLoS One* 9(2):e87737.
- 531 13. Munro C, et al. (2018) Improved phylogenetic resolution within siphonophora
532 (cnidaria) with implications for trait evolution. *Molecular Phylogenetics and Evolution*.
- 533 14. Damian-Serrano A, Haddock SH, Dunn CW (2019) The evolution of siphonophore
534 tentilla as specialized tools for prey capture. *bioRxiv*:653345.
- 535 15. Mariscal RN (1974) Nematocysts.
- 536 16. Werner B (1965) Die nesselkapseln der cnidaria, mit besonderer berücksichtigung der
537 hydriida. *Helgoländer wissenschaftliche Meeresuntersuchungen* 12(1):1.
- 538 17. Winemiller KO, Fitzgerald DB, Bower LM, Pianka ER (2015) Functional traits,
539 convergent evolution, and periodic tables of niches. *Ecology letters* 18(8):737–751.
- 540 18. Mackie GO, Pugh PR, Purcell JE (1987) Siphonophore Biology. *Advances in Marine*
541 *Biology* 24:97–262.

- 542 19. Purcell J (1981) Dietary composition and diel feeding patterns of epipelagic
543 siphonophores. *Marine Biology* 65(1):83–90.
- 544 20. Harmon LJ, Weir JT, Brock CD, Glor RE, Challenger W (2007) GEIGER: Investi-
545 gating evolutionary radiations. *Bioinformatics* 24(1):129–131.
- 546 21. Sugiura N (1978) Further analysts of the data by akaike's information criterion
547 and the finite corrections: Further analysts of the data by akaike's. *Communications in*
548 *Statistics-Theory and Methods* 7(1):13–26.
- 549 22. Pennell MW, FitzJohn RG, Cornwell WK, Harmon LJ (2015) Model adequacy and the
550 macroevolution of angiosperm functional traits. *The American Naturalist* 186(2):E33–E50.
- 551 23. Blomberg SP, Garland T, Ives AR (2003) Testing for phylogenetic signal in comparative
552 data: Behavioral traits are more labile. *Evolution* 57(4):717–745.
- 553 24. Revell LJ (2012) Phytools: An r package for phylogenetic comparative biology (and
554 other things). *Methods in Ecology and Evolution* 3(2):217–223.
- 555 25. Felsenstein J (1985) Phylogenies and the comparative method. *The American*
556 *Naturalist* 125(1):1–15.
- 557 26. Revell LJ, Chamberlain SA (2014) Rphylip: An r interface for phylip. *Methods in*
558 *Ecology and Evolution* 5(9):976–981.
- 559 27. Adams DC, Collyer M, Kaliontzopoulou A, Sherratt E (2016) Geomorph: Software
560 for geometric morphometric analyses.
- 561 28. Ingram T, Mahler DL (2013) SURFACE: Detecting convergent evolution from
562 comparative data by fitting ornstein-uhlenbeck models with stepwise akaike information
563 criterion. *Methods in ecology and evolution* 4(5):416–425.
- 564 29. Jombart T, Devillard S, Balloux F (2010) Discriminant analysis of principal compo-
565 nents: A new method for the analysis of genetically structured populations. *BMC genetics*
566 11(1):94.
- 567 30. Siebert S, Pugh PR, Haddock SH, Dunn CW (2013) Re-evaluation of characters in
568 apolemiidae (siphonophora), with description of two new species from monterey bay, california.

- 569 *Zootaxa* 3702(3):201–232.
- 570 31. Skaer R (1988) *The formation of cnidocyte patterns in siphonophores* (Academic
571 Press New York).
- 572 32. Skaer R (1991) Remodelling during the development of nematocysts in a siphonophore.
573 *Hydrobiologia* (Springer), pp 685–689.
- 574 33. Blyth CR (1972) On simpson's paradox and the sure-thing principle. *Journal of the
575 American Statistical Association* 67(338):364–366.
- 576 34. Uyeda JC, Zenil-Ferguson R, Pennell MW (2018) Rethinking phylogenetic comparative
577 methods. *Systematic Biology* 67(6):1091–1109.
- 578 35. Bode H (1988) Control of nematocyte differentiation in hydra. *The Biology of
579 Nematocysts* (Elsevier), pp 209–232.
- 580 36. David CN, et al. (2008) Evolution of complex structures: Minicollagens shape the
581 cnidarian nematocyst. *Trends in genetics* 24(9):431–438.
- 582 37. Carré D (1972) Study on development of cnidocysts in gastrozooids of muggiaeae kochi
583 (will, 1844) (siphonophora, calycophora). *Comptes Rendus Hebdomadaires des Seances de
584 l'Academie des Sciences Serie D* 275(12):1263.
- 585 38. Wagner GP (1996) Homologues, natural kinds and the evolution of modularity.
586 *American Zoologist* 36(1):36–43.
- 587 39. Purcell JE (1984) The functions of nematocysts in prey capture by epipelagic
588 siphonophores (coelenterata, hydrozoa). *The Biological Bulletin* 166(2):310–327.
- 589 40. Thomason J (1988) The allometry of nematocysts. *The Biology of Nematocysts*
590 (Elsevier), pp 575–588.
- 591 41. Carré D, Carré C (1980) On triggering and control of cnidocyst discharge. *Marine &
592 Freshwater Behaviour & Phy* 7(1):109–117.
- 593 42. Hessinger DA (1988) Nematocyst venoms and toxins. *The Biology of Nematocysts*
594 (Elsevier), pp 333–368.
- 595 43. Mitra A (2009) Are closure terms appropriate or necessary descriptors of zooplankton

⁵⁹⁶ loss in nutrient–phytoplankton–zooplankton type models? *Ecological Modelling* 220(5):611–
⁵⁹⁷ 620.